TGFβ signaling pathway is altered by HLA-B27 expression, resulting in pathogenic consequences relevant for spondyloarthritis

Marc Lauraine, Maxence de Taffin de Tilques, Dganit Melamed-Kadosh, Bilade Cherqaoui, Vincent Rincheval, Erwann Prevost, Aurore Rincheval-Arnold, Eneida Cela, Arie Admon, Isabelle Guénal, et al.

TGFβ signaling pathway is altered by HLA-B27 expression, resulting in pathogenic consequences relevant for spondyloarthritis.

Marc Lauraine
Inserm
Maxence De Taffin De Tilques
Versailles Saint-Quentin-en-Yvelines University
Dganit Melamed-Kadosh
Technion – Israel Institute of Technology
Bilade Cherqaoui
Hôpital Ambroise-Paré
Vincent Rincheval
Versailles Saint-Quentin-en-Yvelines University
Erwann Prevost
Versailles Saint-Quentin-en-Yvelines University
Aurore Rincheval-Arnold
Versailles Saint-Quentin-en-Yvelines University
Eneida Cela
University of Rome Tor Vergata
Arie Admon
Technion – Israel Institute of Technology
Isabelle Guénal
Versailles Saint-Quentin-en-Yvelines University
Luiza Araujo
Inserm
Maxime Breban (maxime.breban@aphp.fr)
Hôpital Ambroise-Paré

Research Article

Keywords: Spondyloarthritis, BMP/TGFβ pathway, HLA-B27, CD4 + T cells, peptidome, rat, Drosophila

Posted Date: December 21st, 2023

DOI: https://doi.org/10.21203/rs.3.rs-3749796/v1

Additional Declarations: No competing interests reported.

Abstract

Background

Association of HLA-B27 with spondyloarthritis (SpA) has been known for 50 years, but still remains unexplained. We recently showed that HLA-B27expressed in wing imaginal disc from HLA-B27/human-β2 microglobulin (hβ2m) transgenic *Drosophila* deregulated bone morphogenetic protein (BMP) pathway by interacting physically with type I BMP receptor (BMPR1) Saxophone (Sax), leading to crossveinless phenotype.

Methods

Genetic interaction was studied between activin/transforming growth factor β (TGFb) pathway and HLA-B27/hβ2m in transgenic *Drosophila* wings. The HLA-B27-bound peptidome was characterized in wing imaginal discs. In mesenteric lymph node (mLN) T cells from HLA-B27/hβ2m rat (B27 rat), physical interaction between HLA-B27 and activin receptor-like kinase-2 (ALK2), ALK3 and ALK5 BMPR1s, phosphorylation of small mothers against decapentaplegic (SMADs) and proteins of the non-canonical BMP/TGFb pathways induced by its ligands, and the transcript level of target genes of the TGFb pathway, were evaluated.

Results

In HLA-B27/hβ2m transgenic *Drosophila*, inappropriate signalling through the activin/TGFβ pathway, involving Baboon (Babo), the type I activin/TGFβ receptor, contributed to the crossveinless phenotype, in addition to deregulated BMP pathway. We identified peptides bound to HLA-B27 with the canonical binding motif in HLA-B27/hβ2m transgenic *Drosophila* wing imaginal disc. We demonstrated specific physical interaction, between HLA-B27/hb2m and mammalian orthologs of Sax and Babo, i.e. ALK2 and ALK5 (i.e. TGFb receptor I), in the mLN cells from B27 rat. The magnitude of phosphorylation of SMAD2/3 in response to TGFβ1 was increased in T cells from B27 rats, showing evidence for deregulated TGFb pathway. Accordingly, expression of several target genes of the pathway was increased in T cells from B27 rats, in basal conditions and/or after TGFb exposure, including *Foxp3*, *Rorc*, *Runx1* and *Maf*. Interestingly, *Tgfb1* expression was reduced in naïve T cells from B27 rats, even premorbid, an observation consistent with a pro-inflammatory pattern.

Conclusions

This study shows that HLA-B27 alters the TGFβ pathways in *Drosophila* and B27 rat. Given the importance of this pathway in CD4 + T cells differentiation and regulation, its disturbance could

contribute to the abnormal expansion of pro-inflammatory T helper 17 cells and altered regulatory T cell phenotype observed in B27 rats.

Introduction

Spondyloarthritis (Spa) is a chronic inflammatory rheumatism that can affect axial and/or peripheral skeleton. It typically combines sacroiliitis with spondylitis, which can progress into bone fusion. It may also comprise peripheral arthritis and enthesitis, dactylitis, and extra-articular features, including uveitis, psoriasis, and inflammatory bowel disease (IBD). The HLA-B27 allele of the major Class-I histocompatibility complex (MHC-I) is the genetic factor most strongly associated with SpA, being present in 70–90% of the patients (1).

This striking association was first described 50 years ago but its underlying mechanisms remain incompletely understood (2). Several lines of rats transgenic for HLA-B27 and human β2-microglobulin (hb2m) (B27 rat) were developed to investigate the implication of HLA-B27 in the pathogenesis of SpA. The B27 rats develop spontaneously multisystem inflammatory disorder that resembles human SpA by combining arthritis with IBD and psoriasis and is specific for HLA-B27 as HLA-B7/hb2m transgenic rats remain healthy. Among other advances, this model highlighted the critical role of myeloid derived cells expressing HLA-B27 and CD4 + T cells in disease development (3). In particular, an uncontrolled expansion of pro-inflammatory T helper 17 (Th17) cells and an altered regulatory T cell (Treg) phenotype, depending on deregulated antigen-presenting cells function were evidenced in this model (4–6). In contrast, CD8 + T cells appeared dispensable, arguing against the "arthritogenic" peptide hypothesis, which implicated the canonical antigen-presentation function of the MHC-I molecule.

Recently, we produced a transgenic *Drosophila* expressing HLA-B27 to identify HLA-B27 non-canonical properties that could explain its pathogenicity (3). In this new model, we reported the unexpected interference of HLA-B27 with the bone morphogenetic proteins (BMP)/transforming growth factor beta (TGFβ) pathway. Indeed, when HLA-B27 (but not HLA-B7) was expressed in combination with hb2m in the *Drosophila* wing imaginal discs, it was shown to physically interact as well-folded conformer (recognized by w6/32 antibody (Ab)) with the type I BMP receptor (BMPR1) Saxophone (Sax) and to antagonize its inhibitory function thereby enhancing BMP signaling and leading to a loss of crossveins. Likewise, physical interaction was specifically observed between well-folded conformers of HLA-B27 (recognized by ME1 and w6/32 Abs) and activin receptor-like kinase-2 (ALK2, the Sax mammalian ortholog) in B-lymphoblastoid cell lines (B-LCL) from SpA patients. Moreover, stimulation of T cells from HLA-B27 + SpA patients with both TGFβ and activin-A led to an exacerbated response (7).

The BMP/TGFβ pathway is one of the most pleiotropic signaling pathways. It is involved in embryonic development as well as in adult organisms in various phenomena such as homeostasis, cell migration, and cell proliferation. It is notably implicated in ossification and immune response, two complementary facets of SpA pathology (8). TGFβ1 exerts major effects on the differentiation of naïve CD4 + T cell (Tn), by promoting their differentiation into Treg and Th17 cells (9–11). The right balance between these two

subsets of CD4 + T cells appears critical to prevent several autoimmune/inflammatory diseases including SpA (12). Given the excessive Th17 expansion and altered Treg phenotype that were observed in B27 rats and the critical role of activin/TGFβ signaling in Treg/Th17 differentiation (4, 5), here, we investigated whether activin/TGFβ pathway was altered in HLA-B27 transgenic *Drosophila* and in CD4 + T cells from B27 rats.

Materials and methods

Drosophila crossing and wings preparation.

Fly strains were grown in standard corn/agar medium. Crosses were performed at 25°C. The different fly stocks employed in this study are listed in Supplementary Table 1. Wings were dissected and placed in a glycerol/ethanol drop on a glass slide and imaged at 4X magnification using an Olympus SZX16 stereomicroscope and an Olympus Infinity3 camera. Veins length and wing area were measured with FIJI pixel length and area functions (https://imagej.nih.gov/ij/).

Drosophila wing imaginal discs collection.

Drosophila wing imaginal discs were collected as described in (13). Briefly, this protocol enables the recovery of many wing imaginal discs by grinding a large quantity of *Drosophila* larvae followed by organs separation using filtration and a density gradient. To ensure sufficient HLA-B27 recovery after affinity purification for high-quality bound-peptides analysis, we determined that approximately $2x10^8$ cells expressing HLA-B27 were necessary. As imaginal wing disc contains 50,000 cells and 60% of imaginal wing disc cells express HLA-B27 (7), 7,000 nub > HLA-B27 and 4,000 wild-type *Drosophila* wing imaginal discs were collected. Collected wing imaginal discs were frozen at -80°C and sent to the Technion-Israel Institute of Technology for HLA-B27-bound peptidome identification.

Affinity purification of the HLA molecules and analysis of the bound peptides.

Total proteins were extracted from wing imaginal discs and the HLA molecules were immunoaffinity-purified using the w6/32 mAb, which recognizes HLA-A, B, and C well-folded heavy chain- covalently linked to AminoLink-agarose resin (Thermo Fisher Scientific, Rockford, IL) as described previously (14). The HLA molecules with their bound peptides were eluted from the beads with 1% trifluoroacetic acid (TFA), which also induces dissociation of the HLA-β2m peptide complexes. The released peptides were separated from the HLA heavy subunit, the β2m, and from other bound proteins using disposable reversed-phase MicroTip C18 columns (Harvard Apparatus, Holliston, MA) and eluted with 30% acetonitrile and 0.1% TFA, as described previously (15) while the HLA heavy chain, β2m, and other bound proteins were recovered with 30% acetonitrile and 0,1% TFA. The peptides were partially resolved by a capillary high-performance liquid chromatography (HPLC) on pulled capillaries of 0.075-mm inner diameter and about 20 cm long (16) packed with C18 reversed-phase 3.5-µm beads (Reprosil-C18-Aqua, Dr. Maisch GmbH, Ammerbuch-Entringen, Germany). Chromatography was performed with the UltiMate 3000 RSLC nano-capillary UHPLC system (Thermo Fisher Scientific), which was coupled by electrospray

to tandem mass spectrometry (MS) on Q-Exactive-Plus (Thermo Fisher Scientific), using the same parameters as in Bourdetsky et al., 2014). The HLA peptides were eluted with a linear gradient over 2 hours from 5 to 28% acetonitrile with 0.1% formic acid at a flow rate of 0.15 µl/min. Data were acquired using a data-dependent 'top 10' method, fragmenting the peptides by higher energy collisional dissociation (HCD). The full scan MS spectra were acquired at a resolution of 70,000 at 200 m/z with a target value of 3 x 10^6 ions. Ions were accumulated to AGC target value of 10^5 with a maximum injection time of 100 millisec. No fragmentation was performed for peptides with unassigned precursor ion charge states or charge states of four and above. The peptide match option was set to Preferred. Normalized collision energy was set to 25%, and MS/MS resolution was set to 17,500 at 200 m/z. Fragmented masses were dynamically excluded from further selection for fragmentation for 20 s.

The protein fraction eluted from the affinity column was eluted from the same reversed-phase column with 80% acetonitrile. The eluted protein fractions were dried by vacuum centrifugation, dissolved 8 M urea (Sigma-Aldrich), 400 mM ammonium bicarbonate (Sigma-Aldrich) and 10 mM dithiothreitol (Sigma-Aldrich). Half of the sample was reduced at 60°C for 30 min. Carbamidomethylation was performed in the dark for 30 min by 40 mM iodoacetamide (IAA, Sigma-Aldrich). Next, three volumes of HPLC water were added, followed by 0.2 µg trypsin (Promega, Madison, Wisconsin, USA) and an overnight incubation at 37℃. Another aliquot of 0.2 µg trypsin was added and incubated for 3 hours at 37°C. The digested samples were acidified to a final concentration of 0.1% TFA and desalted on C18 StageTips prior to MS analysis. The tryptic peptides from the 80% acetonitrile fraction described above were analyzed in liquid chromatography (LC)-MS/MS using Q Exactive HF mass spectrometer (Thermo) fitted with a capillary HPLC easy nLC 1200 (Thermo-Fisher Scientific). The peptides were loaded in solvent A (0.1% formic acid in water) on a homemade capillary column (30 cm, 75-micron ID) packed with Reprosil C18-Aqua (Dr. Maisch GmbH, Germany). The peptides mixture was resolved with a 5 to 28% linear gradient of solvent B (80% acetonitrile with 0.1% formic acid) for 120 minutes followed by a gradient of 15 minutes of 28 to 95% and 15 minutes at 95% acetonitrile with 0.1% formic acid in water at flow rates of 0.15 µl/min. Mass spectrometry was performed in a positive mode (m/z 300–1800, resolution 60,000 for MS1 and 15,000 for MS2) using repetitively full MS scan followed by HCD fragmentation at 27 normalized collision energy of the 10 most dominant ions with two and above charges selected from the first MS scan. The AGC settings were 3x106 for the full MS and 1x105 for the MS/MS scans. The intensity threshold for triggering MS/MS analysis was 1x104. A dynamic exclusion list was enabled with an exclusion duration of 20 seconds.

Peptidome data analysis.

Peptides were identified and quantified using the MaxQuant software tool (18) version 1.6.17.0 with the Andromeda (19) search engine using the *Drosophila melanogaster* section of the UniProt/Swiss-Prot database (release Jan 29, 2021, containing 22,114 entries, 13,821 genes). HLA peptides were identified in the database assuming no specific enzyme proteolysis. Methionine oxidation and N-acetylation were accepted as variable modifications. The peptide precursors and fragment mass tolerances were set at 6 and 20 ppm, respectively. The minimal peptide length was set to eight amino acid residues. The false

discovery rate (FDR) was set, separately, for 0.05 for HLA peptides. The 'match between runs' subroutine was used in the analysis. MaxQuant quantifies the relative signal intensities of the peptides using their LC-MS peak volumes. Graphical and statistical analyses of the results were performed with Perseus (20). Assignment of HLA scores to the different identified peptides was done by NetMHC, which ranks the peptides according to their fitness to one of the HLA allomorphs, with peptides ranking below 2% relative to 400,000 different peptides in the NetMHC database considered as intermediate affinity ligands of the particular HLA (21, 22).

The raw MS files of the trypsin-digested protein (80% acetonitrile) fractions were also analyzed by MaxQuant version 1.6.3.4 and searched with the Andromeda search engine using the HLA-B27 and human β2m sequences added to the Drosophila melanogaster section of the UniProt/Swiss-Prot database. The search settings were trypsin-specific, with FDR set to 0.01 and decoy mode Revert. Methionine oxidation and N-acetylation were accepted as variable modifications, while carbamidomethylation of cysteines was accepted as a fixed modification. Intensity-based absolute quantification (iBAQ) was used to quantify the levels of purified HLA-peptide complexes.

The MS peptidomics and proteomics data have been deposited to the ProteomeXchange Consortium (23) (http://proteomecentral.proteomexchange.org) via the PRIDE partner repository with the dataset identifier PXD047119.

Rats.

The SpA-prone B27 rats of the 33 − 3 line bearing 55 copies of HLA-B*2705 and 28 copies of hβ2m and the healthy B7 rats of the 120-4 line bearing 52 copies of HLA-B*0702 and 26 copies of hβ2m, all on a Fisher (F344) background, were bred under conventional conditions (24). Age-matched nontransgenic (NTG) littermates were used as controls. Rats were used at 2 distinct ages: (i) 3–5 wk, asymptomatic, so-called premorbid; (ii) 1,5–12 mo, adults presenting disease symptoms. Study procedures were approved by the Institutional Animal Experimentation Ethical Committee from the Faculty of Health Simone Veil (APAFIS-8910).

Rat cells preparation.

Single-cell suspensions were prepared from mesenteric lymph nodes (mLN), stained with appropriate Abs and analyzed by flow cytometry with BD LSR Fortessa. In some experiments, total T cell population was gated using anti-CD3 antibody (Ab) (Fig. S1C). In other experiments, appropriate combinations of Abs were used to identify and/or sort Tn (CD4 + CD25-CD62L^{high}) and effector CD4 + T cells (Teff; CD4 + CD25-CD62L-) (Fig. S1D).

Proximity ligation assay.

Proximity ligation assay (PLA) was performed using Duolink In Situ PLA reagents from Merck (Red detection reagent duo 92008/Probe Anti-Rabbit PLUS 92002/Probe Anti-Mouse MINUS 92004) following

the manufacturer's protocol. For each experiment, 3 x 10^5 total mLN cells were used. Primary Abs w6.32 (Abcam) and CD45RC (Bio-rad) are produced in mice, anti- ALK2 (Sigma-Aldrich), anti- ALK3 (Invitrogen) and anti- ALK5 (Sigma-Aldrich) are produced in rabbit. They were all used at 1:100 except for ALK5 that was used at 1:150. Whole volume of approximately 10 random fields of view were acquired with 63x oil immersion objective of Leica SP8 confocal microscope using the DAPI (blue nuclei) and TexasRed (Red PLA signal) filters. PLA signal was manually counted in each individual cell and for each Z field using LasX software.

Cell culture reagents and monoclonal Abs (mAbs). Recombinant human TGFβ1(rhTGFβ1), rhBMP-4 and rhBMP-6 were purchased from Mitenyi Biotec. Recombinant human/mouse/rat r(h/m/r) activin A was obtained from R&D Systems. Mouse anti-rat CD3 and mouse anti-rat CD28 Ab were from BD pharmingen. For surface staining, fluorochrome conjugated anti-rat CD3 and anti-rat CD4 were from BD Pharmingen; anti-rat CD4, anti-rat CD25 were obtained from eBioscience and anti-rat CD62L was from Invitrogen. For intracellular staining, fluorochrome conjugated anti-pSMAD2/3 and anti-pSMAD1/8 were from BD Bioscience; anti-pAKT and anti-pNF-κB from Cell Signaling; anti-pERK1/2 and anti-pp38 from Invitrogen. All reagents and Abs used are listed in Supplementary Table 2.

RT-qPCR. Tn and Teff from NTG and B27 rats were collected in TRIzol RNA Isolation Reagents (ThermoFisher), then RNA was extracted using classic chloroform/isopropyl alcohol extraction protocol. cDNA was synthesized by reverse transcription using RevertAid First Strand cDNA Synthesis Kit (ThermoFisher) with polyA primers, then real time quantitative polymerase chain reaction (RT-qPCR) was performed using SsoAdvanced™ Universal SYBR® Green Supermix (BioRad) and CFX384 (Touch Real-Time PCR Detection System). Duplicates were run for each sample; *Gapdh* was used as endogenous reference gene for mRNA abundance normalization. Primer sequences are provided in Supplementary Table 3.

Cell stimulation. Single-cell suspensions (10^6 cells) from mLN were stimulated with TGFβ1 (5ng/ml) or PBS for 1 hour at 37°C/5% CO2. In experiments using sorted-cells, the stimulation was performed on single-cell suspension (5.10^5 or 10^6 cells) after 1 hour of cell resting.When sorted, cells were left to rest at 37°C/5% CO2 for 1 hour.

SMAD2/3, p38, AKT, ERK, mTOR, NFκB phosphorylation assessment by flow cytometry. Single-cell suspension or sorted CD4 + T cell subsets isolated from NTG or B27 rats mLN, were stimulated or not with TGFβ1 for 1 hour as described previously. After stimulation, the cells were fixed for 20 minutes in Fix Buffer I (BD Bioscience) and then permeabilized for 20 minutes in Perm Buffer III (BD Bioscience) at -20°C. Intracellular staining with specific Abs was performed for 1 hour in Perm Wash 1x according to the manufacturer's instructions (BD Bioscience). Unstimulated and unsorted, cells were fixed immediately after isolation. Results were expressed as staining index (SI) calculated as the ratio between samples and fluorescence-minus-one staining control.

Statistical analysis. Data are expressed as the mean ± SEM. Kruskal-Wallis test, followed by Dunn's multiple comparisons tests comparing each condition to its control was used to analyse *Drosophila* experiments. Chi-2 test was used to compare the second position residue between peptides specific for B27 drosophila and those non-specific. Paired t-tests or Fischer's LSD tests were used to analyse flow-cytometry experiments. Unpaired t-tests were used for qPCR experiments. Analyse of variance (ANOVA) followed by unpaired t-test after Bonferroni correction was used for PLA experiment. Results were considered significant when p value was ≤ 0.05.

Results

HLA-B27 interacts genetically with the activin/TGFb pathway in Drosophila. We previously reported that HLA-B27, when expressed in combination with hβ2m in *Drosophila* wing imaginal disc, physically interacted with BMPR1 saxophone (Sax) leading to an increased BMP signaling and a loss of crossveins (7). Given the possible interplay between BMP and activin/TGFb pathways that signal *via* Thickveins (Tkv)*/*Sax and baboon (Babo) BMPR1s, respectively, we further investigated the involvement of the latter pathway in the loss of crossveins induced by HLA-B27/hβ2m expression. Down regulation of the ligand of the pathway, *activin*, or its BMPR1, *Babo*, or its signal transducer *Smox* using RNA interference (RNAi) do not affect wing formation in wild-type *Drosophila* (Fig. 1A,C,E,G). However, in B27/hβ2m *Drosophila*, it leads to a full or partial rescue of the crossveins, confirming a genetic interaction between HLA-B27 and the activin pathway in addition to the BMP pathway (Fig. 1B,D,F,H,I). Altogether, this indicates that in the presence of HLA-B27, inappropriate activin/TGFb signaling participated to the loss of crossveins.

Well-folded conformers of HLA-B27/hb2m loaded with canonical peptides are expressed in transgenic Drosophila wing imaginal disc. In our previous work, we showed that HLA-B27 folded and localized to the cell membrane in *Drosophila* wing imaginal disc. Its recognition by ME1 Ab suggested that the HLA-B27 peptide-binding groove was not empty (7). To further address this question, we collected wing imaginal discs from *Drosophila* expressing HLA-B27/hβ2m. Wild-type wing imaginal discs were used as control. Immunoaffinity purification of HLA-B27 molecule was performed with w6/32 antibody, followed by large scale quantitative MS to identify HLA-B27-specific peptide ligands. In this assay, both HLA-B27 and hβ2m molecules were purified from the HLA-B27/hβ2m *Drosophila* wing disc and absent from the wild-type condition (according to the proteome analysis of the 80% acetonitrile fraction, showing clear identification and quantification of both proteins). Furthermore, peptidome analysis identified 50 peptides specific for HLA-B27 (Fig. 1J, left panel) with 56% presenting an arginine (50%) or a glutamine (6%) at the anchor position 2, a hallmark of HLA-B27 peptide-binding motif (Fig. 1J, right panel). These peptides are longer on average than those usually purified from mammalian cells with a majority spanning 10 to 11 amino acid residues (61%) and < 1% having the canonical 9 amino acids in length. Altogether these findings indicate that HLA-B27 associates with both hβ2m and specific peptides in *Drosophila* despite the lack of the peptide loading complex and ERAP aminopeptidase, which might explain the longer than usual length of those peptides, as previously shown (25). The *Drosophila* proteins and functions corresponding to these peptides are shown in Table 1. Noteworthy, a comparison of HLA-B27-bound *Drosophila* peptides with previously reported HLA-B27 peptidome from human or B27 rat cells revealed

only one rat peptide overlapping with one of the *Drosophila* peptides (TEAPLNPKAN), both derived from actin. However, in the rat, it was not specific for the HLA-B27-bound peptidome (25, 26).

Table 1
HLA-B27-specific peptides in *Drosophila* with their corresponding protein and implication in biological process.

Peptide	Protein	Biological process
APGSGAPG	Trailer hitch, isoform E	**Cytoskeleton**
EEQEAEVDEN	Tubulin beta-1 chain	
GRPLVTMSTY	Uncharacterized protein, isoform E	
LEELQQENCR	Augmin complex subunit dgt3	
TEAPLNPKAN*	Actin-5C	
NRLMYSVIGATEY; VQYDPRNSETY	Z band alternatively spliced PDZ-motif protein 66, isoform I	
VRYQQQQQQQQQY	Z band alternatively spliced PDZ-motif protein 52, isoform R	
AQGDFNEFIEK	Neuropeptide-like 2	**Immunity**
ARNDPQDDAE; ARNDPQDDAEVIK	GH02216p	
GRITTNQDR; QRAMNPVMSI	Fat-body protein 1, isoform D	
SRMEYSFSNGVVTQ	Sidestep III, isoform O	
SRLTYGSNA; SRLTYGSNAASTF; SSRLTYGSNAASTF	Fondue, isoform A	
ARAEINFEGPSP; ARAEINFEGPSPA	BcDNA.GH11973	**DNA/RNA**
ARPYQPDGYQY	RE50839p	
NGEFGNELPQRQ	Vig2, isoform B	
STITSREIQ	Histone H2B	
SVNQQSKTQTVSN	Protein lingerer, isoform L	
AAKQTGPIVIS	40S ribosomal protein S19a (Ribosomal protein S19a, isoform C)	**Translation**
AGDSKANPPKGAA; EEIKKEVSS; GQIANGYTPV	Elongation factor 1-alpha	

Flybase website was used to determine the corresponding proteins and biological process (flybase.org).

*This peptide was shared with the HLA-B27-bound peptidome isolated from B27-rats spleen but was not specific for HLA-B27 (25).

Peptide	Protein	Biological process
NPNQQSERP	Eukaryotic translation initiation factor 4H1, isoform A	
VRIGQPIMSV	60S ribosomal protein L10	
DGSVGPVGP; DGSVGPVGPAGP	Nicotinic acetylcholine receptor alpha7, isoform A	**Ion transport**
HTNNVQEPK	Calsyntenin-1	
TVSGVNGP	V-type proton ATPase subunit B (Vacuolar proton pump subunit B)	
YSKTKSAAPNFDE	GEO09626p1	
EGVEGIEHQE	Protein GDAP2 homolog	**Stress response**
IEQAGKDATEN	Cytochrome b5	
TEDASHMEEVD	Heat shock protein 83	
ERNQNGEDVVK	FI19426p1	**Membrane receptor**
QRVGITAEDL	Msr-110, isoform D	
YRNAGLYNGNT; YRNAGLYNGNTL; YRNAGLYNGNTLVD	GM18993p	
GRSNISFATSP	Nucleoporin NUP53	**Nuclear membrane**
APSGGPAG	HECT-type E3 ubiquitin transferase	**Ubiquitylation**
GRGNIGQTNY	3-oxoacyl-[acyl-carrier-protein] reductase	**Fatty acid metabolism**
SRAPGGAGTGGM	Protein transport protein Sec61 subunit beta	**Autophagy/ Intracellular protein transport**
GPGAGPGQRP	FI16123p1	**Unknown**
MRVPPYYLLM; MRVPPYYLLMQ	Uncharacterized protein, isoform A	
YRIIESNEVPK	Uncharacterized protein	

Flybase website was used to determine the corresponding proteins and biological process (flybase.org).

*This peptide was shared with the HLA-B27-bound peptidome isolated from B27-rats spleen but was not specific for HLA-B27 (25).

HLA-B27 interacts with ALK2 and ALK5 in B27 rat. The mammalian orthologs of the three *Drosophila* BMPR1s, Sax, Tkv and Babo are ALK2, ALK3 and ALK5, respectively. They are primarily involved in BMP (ALK2 and ALK3) and Activin/TGFb (ALK5, also known as TGFbR1) signaling, respectively. We have previously shown a specific physical interaction between HLA-B27 and ALK2 in B-LCLs derived from SpA patients. Here, we wished to investigate the physical interaction between HLA-B27 and ALK2, ALK3 and ALK5 in B27 rat mLN cells, using PLA and HLA-B7 transgenic rats as control. This assay revealed a significantly greater interaction of ALK2 and ALK5 with HLA-B27 than HLA-B7 (Fig. 2B,D,F,H,I). In contrast, the level of interaction of ALK3 with both HLA-B molecules was similar (Fig. 2C,G,I). The PLA signal between ALKs and irrelevant CD45RC protein was comparable to background (Fig. 2A,E,I). These PLA results could not be explained by variations in the levels of expression of HLA-B27 and HLA-B7 which were similar in both lines of rats (27). Moreover, the levels of expression of the different BMPRs were similar between B27 and control rats, except for a decreased expression of *Bmpr1a* that codes for ALK3 in Tn and an increase of *Bmpr2* in Teff from B27 rat (Fig. 3).

TGFβ induces heightened phosphorylation of SMAD2/3 in T cells from B27 rat.

To test whether the BMP/TGFβ pathway was affected by expression of HLA-B27 in adult rat, we stimulated bulk mLN cells or sorted CD4 + T cell subsets with BMPs (2, 4 or 6), activin A or TGFβ1. BMPs failed to induce the phosphorylation of SMAD1/5/8 in rat T cells after different doses and timing of exposure (Supplementary Fig. 1A). Likewise, activin A had a very little or no effect on rat T cells (Supplementary Fig. 1B). In contrast, TGFβ1 increased SMAD2/3 phosphorylation in all mLN T cell subsets. The phosphorylation of SMAD2/3 in CD3 + T cells was significantly lower in unstimulated mLN cells from adult B27 rats and higher after TGFβ1 treatment (Fig. 4A; Supplementary Fig. 1C,F), an observation similar to what we already reported in peripheral blood T cells from SpA patients (7). In sorted Tn, the level of SMAD2/3 phosphorylation was also lower in unstimulated cells from adult B27 rats than in NTG rat, but after TGFβ1 treatment, phosphorylation reached comparable levels between NTG and B27 rats (Fig. 4B; Supplementary Fig. 1D). In B27 Teff, SMAD2/3 phosphorylation after stimulation with TGFβ1 almost reached significant difference compared to NTG Teff ($p = 0.06$) (Supplementary Fig. 1D). Thus, the pSMAD2/3-fold change (i.e. TGFβ/PBS ratio) was higher in both Tn and Teff from B27 rats (Fig. 4C and Supplementary Fig. 1F).

We next examined the effect of TGFb1 on SMAD2/3 phosphorylation in mLN T cell subsets from 3 weeks-old premorbid rats to eliminate the impact of chronic inflammation on this response. Again, in medium control conditions, a lower level of SMAD2/3 phosphorylation was observed in Tn but also in Teff from B27 rats compared to their NTG littermates (Fig. 4D, Supplementary Fig. 1E). The level of pSMAD2/3 achieved after TGFβ1 exposure in Tn and Teff was similar between B27 and NTG rat but, as for adult rats, the fold-change was greater in B27 rat (Fig. 4D and Supplementary Fig. 1G).

Besides canonical SMAD2/3 phosphorylation, TGFb may signal through non-canonical pathways. To address the effect of TGFb on these pathways, we tested the phosphorylation of p38, AKT, mTOR, ERK1/2 and NF-κB after TGFβ1 treatment, in gated or sorted mLN T cell subsets from adult and

premorbid B27 rats, in comparison with NTG control rats. Whatever the time of exposure, TGFβ1 failed to induce phosphorylation of any of these proteins (Supplementary Fig. 2A). However, basal phosphorylation of some of them was significantly decreased in several premorbid B27 rat T cell subsets. Thus, the basal levels of p-p38, pAKT, pmTOR, and pERK were significantly lower in Tn and/or Teff from premorbid B27 rats than in NTG littermates (Supplementary Fig. 2B). This was generally not the case in T cells from adult rats.

Differential expression of TGFβ1 target genes in Tn from NTG and B27 rats.

We next addressed whether higher SMAD2/3 phosphorylation amplitude observed after TGFβ1 exposure in several T cell subsets from B27 rats translated into differential target genes induction. Kinetic of target genes transcripts level was quantified in sorted Tn from adult B27 rats and NTG littermates, after exposure to TGFβ1 over 6-hrs. In Tn from adult B27 rats, expression of *Foxp3* and *Rorc*, which are characteristic TGFb target genes, was increased in basal condition but not modified by TGFb1 treatment (Fig. 5A). *Runx1* that codes for a transcription factor implicated in Th17 cell differentiation, in combination with RORgt and FOXP3, reached a significantly higher level of expression in B27 rat, after 1 hr of TGFb1 exposure, coincident with its peak of expression (Fig. 5A). Expression of *Maf* that is also implicated in Th17 cell differentiation was also higher in Tn from B27 than NTG rats with a noticeable peak of expression in B27 Tn after 6 hrs induction. In contrast, two other TGFb target genes, *Smad7*, which codes for an inhibitor of the pathway and *Tgfb1* itself were less induced by TGFb, in B27 than in NTG rat Tn after 1 hr of TGFb1 exposure but reached comparable levels thereafter, which indicates slightly different kinetics of stimulation (Fig. 5A). Given the importance of TGFb itself in controlling inflammation, we investigated the *Tgfb1* expression in *ex-vivo* sorted Tn and revealed a lower expression in both adult and premorbid rats B27 rats compared to NTG rats (Fig. 5B).

Discussion

Using a new model of HLA-B27/hβ2m transgenic *Drosophila* to explore non-canonical effects of HLA-B27 that might explain its pathogenicity, we previously reported an interaction between HLA-B27 and Sax, one of three *Drosophila* BMPR1s. Our previous study showed that HLA-B27 expressed in wing imaginal disc exerted a dominant negative effect on Sax function, limiting BMP signaling during crossveins formation, resulting in a loss of crossveins by enhanced BMP signaling (7). Moreover, HLA-B27 conformers recognized by w6/32 and ME1 Abs were shown to interact physically with Sax in wing imaginal disc and also with its mammalian orthologue ALK2 in B-LCLs from SpA patients.

In the present follow-up study, we first evidenced that the loss of crossveins induced by expression of HLA-B27/hb2m in *Drosophila* wings implicates a deregulated activin/TGFb pathway. Hence, the ligand activin, its BMPR1 receptor Babo and their down-stream transcription factor Smox were all required for the crossveinless phenotype, indicating inappropriate signaling through the activin/TGFb pathway in the presence of HLA-B27/hb2m. This suggests a complex interplay between HLA-B27 and the BMPR1s, which are known to form different combinations of homo or heterodimers with variable outcome (28). In

addition, we evidenced that at least some of the HLA-B27/hb2m conformers purified from the wing imaginal disc with w6/32 Ab were loaded with peptides enriched in canonical B27-binding motif. This may support the conclusion that well-folded HLA-B27 conformers are involved in the wing phenotype. However, the identified peptides did not overlap with previously characterized B27-specific peptidome from human or B27 rat cells. Thus, if the mechanism by which HLA-B27 alters wing formation in *Drosophila* is related to its role in SpA pathogenesis, this is unlikely to involve the binding of defined peptides.

We next turned to the B27 rat to examine the possible implication of BMP/TGFb pathway in SpA pathogenesis. This murine model is characterized by an uncontrolled expansion of pathogenic Th17 cells and a deregulated phenotype of Treg (4, 5). We have recently shown that Tn from B27 rats were prone to develop a pro-inflammatory Th17 phenotype and that this happened even before disease development (29). One of the key mechanisms behind the biased differentiation of B27 rat Tn relied on decreased expression of interferon/Th1-related genes, including *Stat1* and *Tbx21*, that was already apparent in CD4 + single-positive thymocytes from premorbid B27 rats (29). This could account for heightened Th17 differentiation since transcription factors from both pathways cross-regulate each other.

Thus, given the known implication of the BMP/TGFb pathway and particularly of TGFb in the differentiation of CD4 + T cells into Th17 cells, by inhibiting expression of the master transcription factors of Th1 differentiation, including *Tbx21* (9, 30–33) it was interesting to determine if inappropriate signaling *via* this pathway could be the molecular event linking HLA-B27 to the foregoing signature. Possible relevance of such hypothesis was first supported by PLA showing close physical interaction of ALK2 and ALK5, the respective orthologs of Sax and Babo, with HLA-B27/hb2m at the membrane of rat lymph node cells, superior to that with HLA-B7/hb2m, whereas interaction of ALK3 with both HLA-B alleles was comparable. However, despite the expression of their type 1 and type 2 receptors at the RNA and/or protein levels in rat T cells, neither BMPs nor activin A induced detectable phosphorylation of SMAD1/5/8 or SMAD2/3, respectively. In contrast, TGFb induced canonical SMAD2/3 phosphorylation in rat T cells. We observed consistent decreased basal phosphorylation in B27 rat T cell subsets, whereas phosphorylation increased to a greater extent, reaching at least comparable or greater levels after TGFb1 treatment. Overall, this is suggestive of enhanced TGFb signaling in T cells from B27 rats.

We next examined the putative consequences of these findings on several TGFb target genes and made several interesting observations: two key target genes, i.e. *Foxp3* and *Rorc* were increased in Tn from B27 rats without stimulation but were not further modified until 6 hrs following TGFb exposure, whereas two other genes, *Runx1* and *Maf* were induced to higher levels in Tn from B27 rats with TGFb. This is all the most interesting that the combination of those 4 gene products is critical to determine the fate of Tn, particularly regarding Th17 and Treg differentiation (34, 35). The increased basal levels of the first two could be a consequence of *in vivo* exposure of Tn from B27 rats to TGFb. This interpretation is consistent with our previous epigenomic study of Tn from B27 rats that evidenced *de novo* binding motifs for transcription factors including SMAD3 and SMAD4, that were predicted to preferentially bind to B27 rat-specific superenhancer regions (29). Moreover, ingenuity pathway analysis of RNAseq data from adult

and premorbid B27 Tn cells predicted TGFβ1 as an upregulator of genes differentially expressed as compared to NTG Tn cells ((29) and unpublished data). In turn, the decreased basal phosphorylated state of SMAD2/3 in T cells from B27 rats could be interpreted as the consequence of negative feedback following increased signaling and induction of phosphatases (8, 36). This basal difference could potentially explain delayed induction of *Smad7* and *Tgfb1*in B27 rat T cells after exposure to TGFb. It could possibly also explain that *Tgfb1* transcripts were decreased in *ex vivo* sorted Tn, which could bear direct consequences on the development of SpA, given the critical importance of T cell-produced TGFb1 to prevent chronic inflammation (37).

The precise molecular mechanism by which HLA-B27 may impact BMP/TGFb signaling both in *Drosophila* and mammalian cells is still unknown. However, it is noticeable that hb2m plays a critical role in the development of abnormal phenotype in both animal models that we studied, i.e. the HLA-B27 transgenic *Drosophila* and the B27 rat (3, 7). Interestingly, b2m has been shown to bind and signal through TGFb receptors inducing proinflammatory pathway (38). Thus, it is possible that the propensity of HLA-B27 molecule to interact physically with BMPR1s, including ALK5 could favor signaling by b2m through TGFb receptor.

Abbreviations

SpA Spondyloarthritis

hβ2m Human β-2-microglobulin

B27 rat Rat transgenic for HLA-B27 and hb2m

BMP Bone morphogenetic protein

BMPR1 Type 1 bone morphogenetic protein receptor

Sax Saxophone

TGFβ Transforming growth factor β

mLN Mesenteric lymph nodes

ALK Activin receptor-like kinase

SMAD Small mothers against decapentaplegic

Babo Baboon

IBD Inflammatory bowel disease

MHC-I Class I major histocompatibility complex

Th17 T helper 17

Treg Regulatory T cell

Ab Antibody

B-LCL B-lymphoblastoid cell line

Tn Naive CD4 + T cell

TFA Trifluoroacetic acid

HPLC High-performance liquid chromatography

MS Mass spectrometry

HCD Higher energy collisional dissociation

LC Liquid chromatography

FDR False discovery rate

iBAQ Intensity-based absolute quantification

NTG Nontransgenic

Teff Effector CD4 + T cell

PLA Proximity ligation assay

mAb Monoclonal antibody

rh Recombinant human

rm Recombinant mouse

rr Recombinant rat

RT-qPCR Real-time quantitative polymerase chain reaction

PBS Phosphate buffer saline

SI Stain index

ANOVA Analysis of variance

Tkv Thickveins

RNAi RNA interference

UAS Upstream activating sequence

Declarations

Ethics approval and consent to participate

Study procedures were approved by the Institutional Animal Experimentation Ethical Committee from the Faculty of Health Simone Veil (APAFIS-8910).

Consent for publication

Informed consent was obtained from all participants for publication.

Availability of data and materials

The datasets generated and/or analyzed in this study are available from the corresponding author upon reasonable request.

Competing interests

The authors declare no competing interests.

Funding

This study was funded by the Agence National de la Recherche (ANR) with the project reference ANR-19-CE14-0032.

Authors' contributions

ML, MTT, ARA, AA, IG, LA, and MB designed the study. MTT, EP, VR performed the Activin RNAi experiments in *Drosophila* and the related figure and analyses. ML collected *Drosophila* imaginal wing discs, then DMK and AA resolved HLA-B27-associated peptides and analysed the results. ML performed the major part of the rat experiments, analyses and figures. BC, LA and EC helped in some rat experiments. ML, LA and MB wrote the manuscript. All authors have made an intellectual contribution to the manuscript. All authors read and approved the final manuscript.

References

1. Taurog JD, Chhabra A, Colbert RA. Ankylosing Spondylitis and Axial Spondyloarthritis. Longo DL, editor. N Engl J Med. 2016;374(26):2563–74.
2. Breban M, Costantino F, André C, Chiocchia G, Garchon HJ. Revisiting MHC Genes in Spondyloarthritis. Curr Rheumatol Rep. 2015;17(6):40.

3. Breban M, Glatigny S, Cherqaoui B, Beaufrère M, Lauraine M, Rincheval-Arnold A, et al. Lessons on SpA pathogenesis from animal models. Semin Immunopathol. 2021;43(2):207–19. Available from: http://link.springer.com/10.1007/s00281-020-00832-x
4. Araujo LM, Fert I, Jouhault Q, Labroquère K, Andrieu M, Chiocchia G, et al. Increased production of interleukin-17 over interleukin-10 by treg cells implicates inducible costimulator molecule in experimental spondyloarthritis. Arthritis and Rheumatology. 2014;66(9):2412–22.
5. Glatigny S, Fert I, Blaton MA, Lories RJ, Araujo LM, Chiocchia G, et al. Proinflammatory Th17 cells are expanded and induced by dendritic cells in spondylarthritis-prone HLA-B27-transgenic rats. Arthritis Rheum. 2012;64(1):110–20. Available from: https://onlinelibrary.wiley.com/doi/10.1002/art.33321
6. Beaufrère M, Jacoutot M, Ait Ali Said A, Said-Nahal R, Cosentino G, Rizzo C, et al. Pathogenicity of IL-17 Producing Cells in HLA-B27 Transgenic Rat Model of Spondyloarthritis. American college of rheumatism. 2022; Available from: https://acrabstracts.org/abstract/pathogenicity-of-il-17-producing-cells-in-hla-b27-transgenic-rat-model-of-spondyloarthritis/
7. Grandon B, Rincheval-Arnold A, Jah N, Corsi JM, Araujo LM, Glatiny S, et al. HLA-B27 alters BMP/TGFβ signalling in Drosophila, revealing putative pathogenic mechanism for spondyloarthritis. Ann Rheum Dis. 2019;1–10.
8. Massagué J. TGFβ signalling in context. Nat Rev Mol Cell Biol. 2012;13(10):616–30. Available from: https://www.nature.com/articles/nrm3434
9. Veldhoen M, Hocking RJ, Atkins CJ, Locksley RM, Stockinger B. TGFbeta in the context of an inflammatory cytokine milieu supports de novo differentiation of IL-17-producing T cells. Immunity. 2006;24(2):179–89. Available from: http://www.ncbi.nlm.nih.gov/pubmed/16473830
10. Huber S, Schramm C, Lehr HA, Mann A, Schmitt S, Becker C, et al. Cutting edge: TGF-beta signaling is required for the in vivo expansion and immunosuppressive capacity of regulatory CD4 + CD25 + T cells. J Immunol. 2004;173(11):6526–31. Available from: http://www.ncbi.nlm.nih.gov/pubmed/15557141
11. Wang J, Zhao X, Wan YY. Intricacies of TGF-β signaling in Treg and Th17 cell biology. Cell Mol Immunol. 2023; Available from: https://www.nature.com/articles/s41423-023-01036-7
12. Lee GR. The Balance of Th17 versus Treg Cells in Autoimmunity. Int J Mol Sci. 2018;19(3). Available from: http://www.ncbi.nlm.nih.gov/pubmed/29510522
13. Hoareau M, de Noiron J, Colin J, Guénal I. Mass Purification Protocol for Drosophila melanogaster Wing Imaginal Discs: An Alternative to Dissection to Obtain Large Numbers of Disc Cells. Biology (Basel). 2022;11(10):1384. Available from: https://www.mdpi.com/2079-7737/11/10/1384
14. Bassani-Sternberg M, Barnea E, Beer I, Avivi I, Katz T, Admon A. Soluble plasma HLA peptidome as a potential source for cancer biomarkers. Proceedings of the National Academy of Sciences. 2010;107(44):18769–76. Available from: https://pnas.org/doi/full/10.1073/pnas.1008501107
15. Milner E, Gutter-Kapon L, Bassani-Strenberg M, Barnea E, Beer I, Admon A. The Effect of Proteasome Inhibition on the Generation of the Human Leukocyte Antigen (HLA) Peptidome. Molecular & Cellular

Proteomics. 2013;12(7):1853–64. Available from: https://linkinghub.elsevier.com/retrieve/pii/S153594762032555X

16. Ishihama Y, Rappsilber J, Andersen JS, Mann M. Microcolumns with self-assembled particle frits for proteomics. J Chromatogr A. 2002;979(1–2):233–9. Available from: https://linkinghub.elsevier.com/retrieve/pii/S0021967302014024
17. Bourdetsky D, Schmelzer CEH, Admon A. The nature and extent of contributions by defective ribosome products to the HLA peptidome. Proceedings of the National Academy of Sciences. 2014;111(16). Available from: https://pnas.org/doi/full/10.1073/pnas.1321902111
18. Cox J, Mann M. MaxQuant enables high peptide identification rates, individualized p.p.b.-range mass accuracies and proteome-wide protein quantification. Nat Biotechnol. 2008;26(12):1367–72. Available from: http://www.ncbi.nlm.nih.gov/pubmed/19029910
19. Cox J, Neuhauser N, Michalski A, Scheltema RA, Olsen J V, Mann M. Andromeda: a peptide search engine integrated into the MaxQuant environment. J Proteome Res. 2011;10(4):1794–805. Available from: http://www.ncbi.nlm.nih.gov/pubmed/21254760
20. Tyanova S, Temu T, Sinitcyn P, Carlson A, Hein MY, Geiger T, et al. The Perseus computational platform for comprehensive analysis of (prote)omics data. Nat Methods. 2016;13(9):731–40. Available from: https://www.nature.com/articles/nmeth.3901
21. Andreatta M, Nielsen M. Gapped sequence alignment using artificial neural networks: application to the MHC class I system. Bioinformatics. 2016;32(4):511–7. Available from: https://academic.oup.com/bioinformatics/article/32/4/511/1744469
22. Nielsen M, Lundegaard C, Worning P, Lauemøller SL, Lamberth K, Buus S, et al. Reliable prediction of T-cell epitopes using neural networks with novel sequence representations. Protein Sci. 2003;12(5):1007–17. Available from: http://www.ncbi.nlm.nih.gov/pubmed/12717023
23. Vizcaíno JA, Csordas A, del-Toro N, Dianes JA, Griss J, Lavidas I, et al. 2016 update of the PRIDE database and its related tools. Nucleic Acids Res. 2016;44(D1):D447–56. Available from: https://academic.oup.com/nar/article-lookup/doi/10.1093/nar/gkv1145
24. Fert I, Cagnard N, Glatigny S, Letourneur F, Jacques S, Smith JA, et al. Reverse interferon signature is characteristic of antigen-presenting cells in human and rat spondyloarthritis. Arthritis and Rheumatology. 2014;66(4):841–51.
25. Barnea E, Kadosh DM, Haimovich Y, Satumtira N, Dorris ML, Nguyen MT, et al. The human leukocyte antigen (HLA)-B27 peptidome in vivo, in spondyloarthritis-susceptible HLA-B27 transgenic rats and the effect of Erap1 deletion. Molecular and Cellular Proteomics. 2017;16(4):642–62.
26. Ben Dror L, Barnea E, Beer I, Mann M, Admon A. The HLA–B*2705 peptidome. Arthritis Rheum. 2010;62(2):420–9. Available from: https://onlinelibrary.wiley.com/doi/10.1002/art.27257
27. Hacquard-Bouder C, Falgarone G, Bosquet A, Smaoui F, Monnet D, Ittah M, et al. Defective Costimulatory Function Is a Striking Feature of Antigen-Presenting Cells in an HLA-B27-Transgenic Rat Model of Spondylarthropathy. Arthritis Rheum. 2004;50(5):1624–35.

28. Massagué J. TGF-beta signal transduction. Annu Rev Biochem. 1998;67:753–91. Available from: http://www.ncbi.nlm.nih.gov/pubmed/9759503
29. Cherqaoui B, Crémazy F, Lauraine M, Shammas G, Said-Nahal R, Mambu Mambueni H, et al. STAT1 deficiency underlies a proinflammatory imprint of naive CD4 + T cells in spondyloarthritis. Front Immunol. 2023;14. Available from: https://www.frontiersin.org/articles/10.3389/fimmu.2023.1227281/full
30. Gorelik L, Constant S, Flavell RA. Mechanism of Transforming Growth Factor β–induced Inhibition of T Helper Type 1 Differentiation. J Exp Med. 2002;195(11):1499–505. Available from: https://rupress.org/jem/article/195/11/1499/39416/Mechanism-of-Transforming-Growth-Factor-induced
31. Wu B, Zhang S, Guo Z, Bi Y, Zhou M, Li P, et al. The TGF-β superfamily cytokine Activin-A is induced during autoimmune neuroinflammation and drives pathogenic Th17 cell differentiation. Immunity. 2021;1–16. Available from: https://doi.org/10.1016/j.immuni.2020.12.010
32. Manel N, Unutmaz D, Littman DR. The differentiation of human TH-17 cells requires transforming growth factor-β and induction of the nuclear receptor RORγt. Nat Immunol. 2008;9(6):641–9. Available from: https://www.nature.com/articles/ni.1610
33. Browning LM, Pietrzak M, Kuczma M, Simms CP, Kurczewska A, Refugia JM, et al. TGF-β–mediated enhancement of T H 17 cell generation is inhibited by bone morphogenetic protein receptor 1α signaling. Sci Signal. 2018;11(545):1–16. Available from: https://www.science.org/doi/10.1126/scisignal.aar2125
34. Zhang F, Meng G, Strober W. Interactions among the transcription factors Runx1, RORγt and Foxp3 regulate the differentiation of interleukin 17–producing T cells. Nat Immunol. 2008;9(11):1297–306. Available from: https://www.nature.com/articles/ni.1663
35. Imbratta C, Hussein H, Andris F, Verdeil G. c-MAF, a Swiss Army Knife for Tolerance in Lymphocytes. Front Immunol. 2020;11. Available from: https://www.frontiersin.org/article/10.3389/fimmu.2020.00206/full
36. Bruce DL, Sapkota GP. Phosphatases in SMAD regulation. Vol. 586, FEBS Letters. 2012. p. 1897–905.
37. Li MO, Wan YY, Flavell RA. T Cell-Produced Transforming Growth Factor-β1 Controls T Cell Tolerance and Regulates Th1- and Th17-Cell Differentiation. Immunity. 2007;26(5):579–91.
38. Hilt ZT, Maurya P, Tesoro L, Pariser DN, Ture SK, Cleary SJ, et al. β2M Signals Monocytes Through Non-Canonical TGFβ Receptor Signal Transduction. Circ Res. 2021;128(5):655–69. Available from: https://www.ahajournals.org/doi/10.1161/CIRCRESAHA.120.317119

Figures

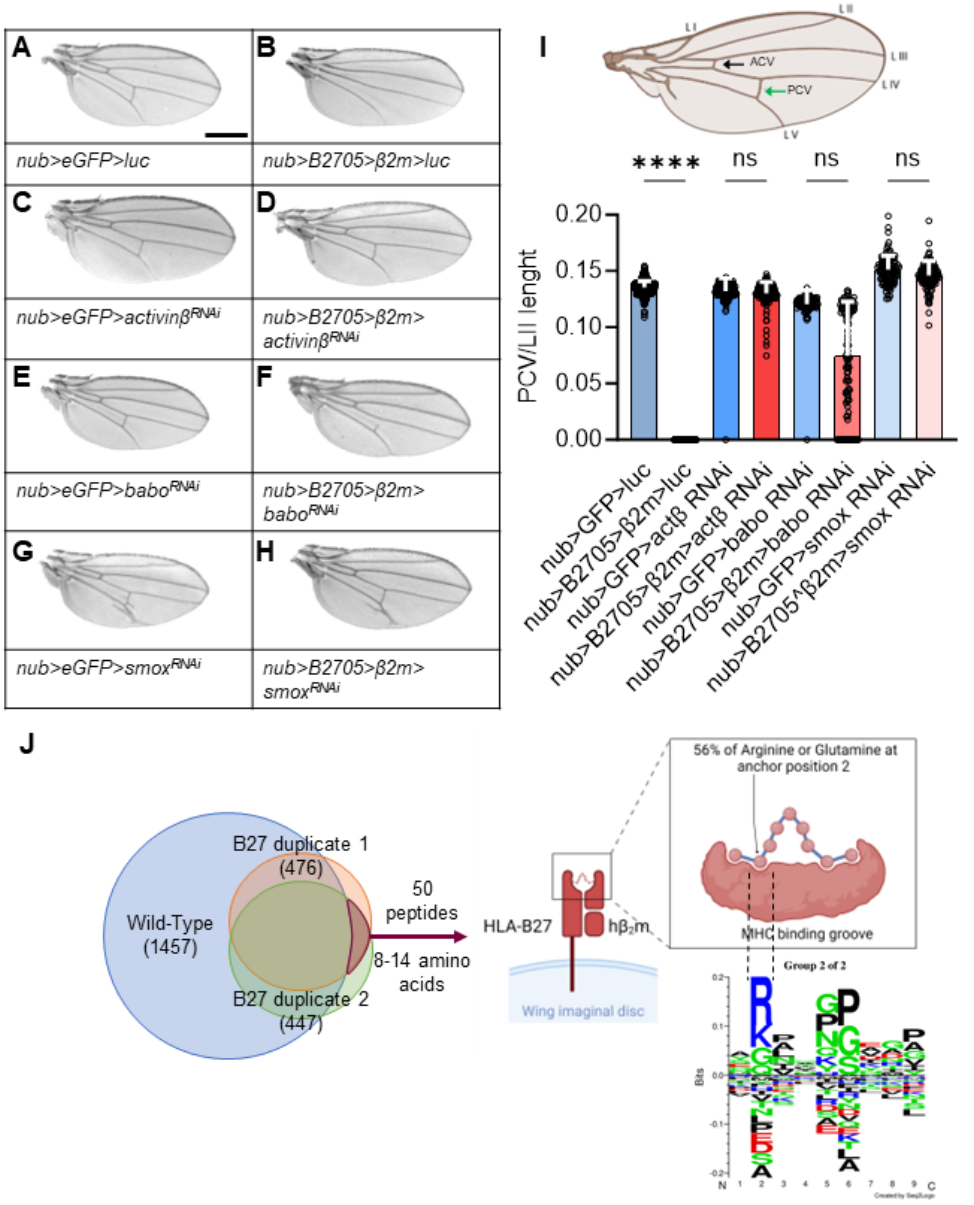

Lauraine et al., Figure 1

Figure 1

HLA-B*27:05/hβ2m expressed in *Drosophila* wing genetically interacts with the activin pathway and binds specific peptidome. (A-H) Nubbin-GAL4 (nub-GAL4) was used to drive transgenes expression in the pouch of imaginal wing disc. Scale bar: 500µm. eGFP and luciferase were used as controls and have no effect on wing formation. Adult fly wings expressing genotypes: (A) nub>enhanced Green fluorescent protein (eGFP)>luciferase (luc) (nub-GAL4/+; UAS-eGFP/UAS-luc), (B) nub>HLA-B27>hβ2m>luc (nub-

GAL4/+; UAS-HLA-B*27:05, UAS-hβ2m/UAS-luc), (C) nub>eGFP>activinβ (actβ) RNA interference (RNAi) (nub-GAL4/+; UAS-eGFP/UAS-actβRNAi), (D) nub>HLA-B27>hβ2m>actβRNAi (nub-GAL4/+; UAS-HLA-B*27:05, UAS-hβ2m/UAS-actβRNAi), (E) nub>eGFP>baboon (babo)RNAi (nub-GAL4/+; UAS-eGFP/UAS-baboβRNAi), (F) nub>HLA-B27>hβ2m>baboRNAi (nub-GAL4/+; UAS-HLA-B*27:05, UAS-hβ2m/UAS-baboRNAi), (G) nub>eGFP>smoxRNAi (nub-GAL4/+; UAS-eGFP/UAS-smoxβRNAi), (H) nub>HLA-B27>hβ2m>smoxRNAi (nub-GAL4/+; UAS-HLA-B*27:05, UAS-hβ2m/UAS-smoxRNAi), (I) Drosophila wing : longitudinal veins (L I to L V), ACV Anterior CrossVein (black arrow), PCV Posterior CrossVein (green arrow), Scatter plot with bar analysis of PCV/LII length ratio, n>80, Kruskal-Wallis followed by Dunn's multiple comparisons test showing only a difference between the control and B*27:05/hβ2m conditions (****: p<0.0001). Vertical error bars represent SD. (J) HLA-B*27:05 from duplicate samples of *Drosophila*wing imaginal discs was retained on immunoaffinity column, using w6/32 Ab. Analysis of the peptides eluted from the column, revealed 50 peptides considered as specifically bound to HLA-B27, as present in both B27 *Drosophila*duplicates and absent from wild-type *Drosophila* wing imaginal disc (left panel). The logo motif (created with GibbsCluster; right panel) shows a high proportion of peptides carrying an Arginine, R or Glutamine, Q in second position that is characteristic of HLA-B27 peptidome (28/50, 56%). A significantly lower proportion of peptides shared between wild-type imaginal discs and B27 duplicates exhibited similar characteristic (28/721, 3.8%; p<0.0001) (figures created with BioRender).

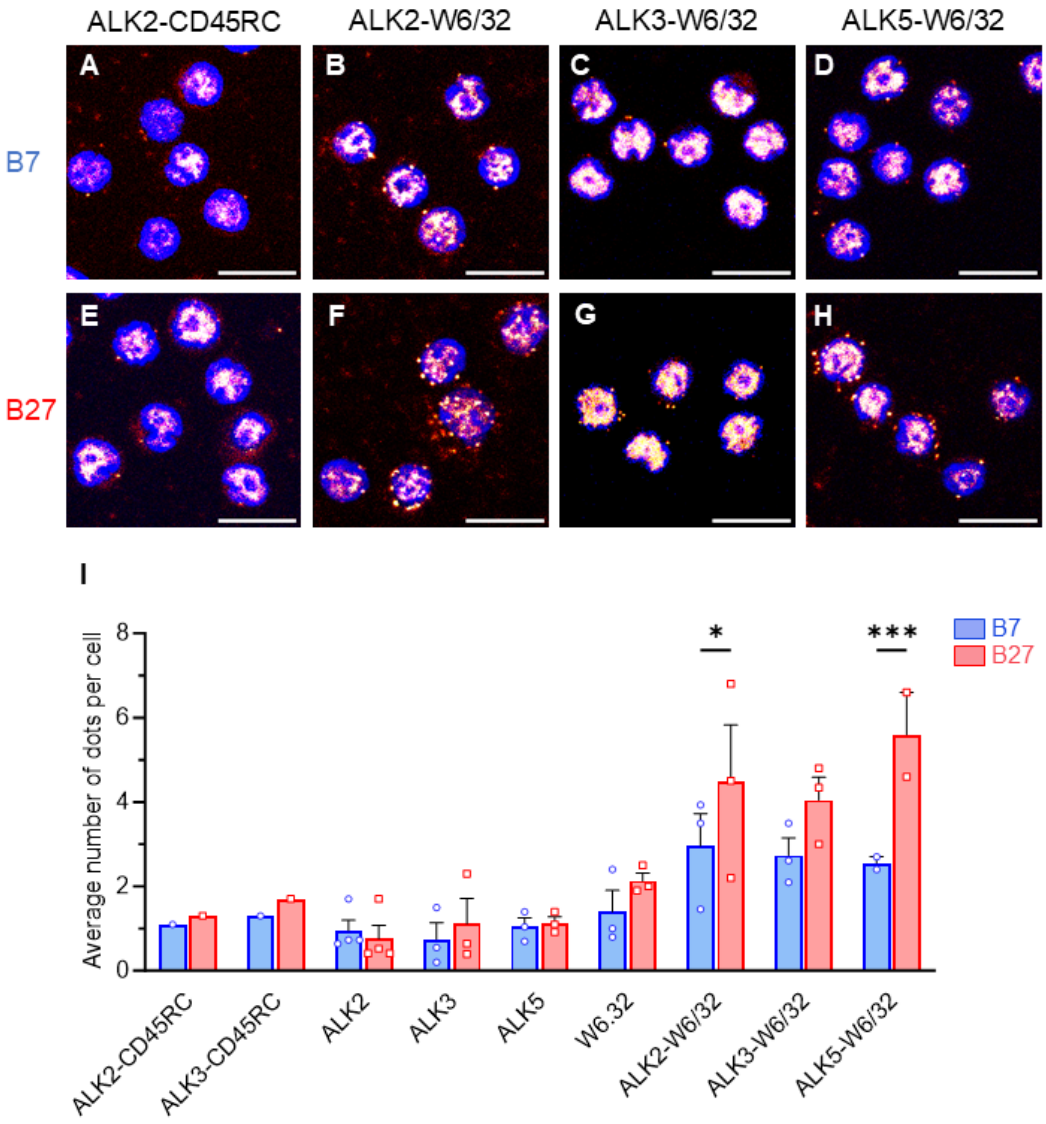

Lauraine et al., Figure 2

Figure 2

HLA-B27 interacts with ALK2 and ALK5 in mLN lymphocytes from B27 rats. PLA was performed on lymphocytes isolated from (A-D) B7 or (E-H) B27 rats mLN, using w6.32 pan MHC-I Ab or anti-CD45RC as control and anti-ALK2, -ALK3 or -ALK5. Images show representative field for each condition. Cells were stained for nuclei (Blue, DAPI) and PLA signal dots (RedHot, PLA kit probes). Scale bar: 10µm. Images were treated with Fiji software. An unspecific PLA signal was homogeneously observed in all conditions.

(I) Average number of PLA staining dots/cell in 2 to 4 independent experiments, showing a greater interaction between ALK2 or ALK5 and HLA-B27 than HLA-B7, whereas interaction was similar for ALK3 with both alleles. The background signal using single Abs was similar to the signal observed by combining anti-ALK Abs with anti-CD45RC. In conditions combining two Abs, approximately 300 to 400 cells per experiment were manually counted, whereas 150 to 250 cells per experiment were manually counted in single Ab conditions. Two-way ANOVA (factors: Ab and rat strain) followed by Bonferroni's multiple-comparisons test was performed (*: p<0.05 ***: p<0.001). Vertical error bars show SEM.

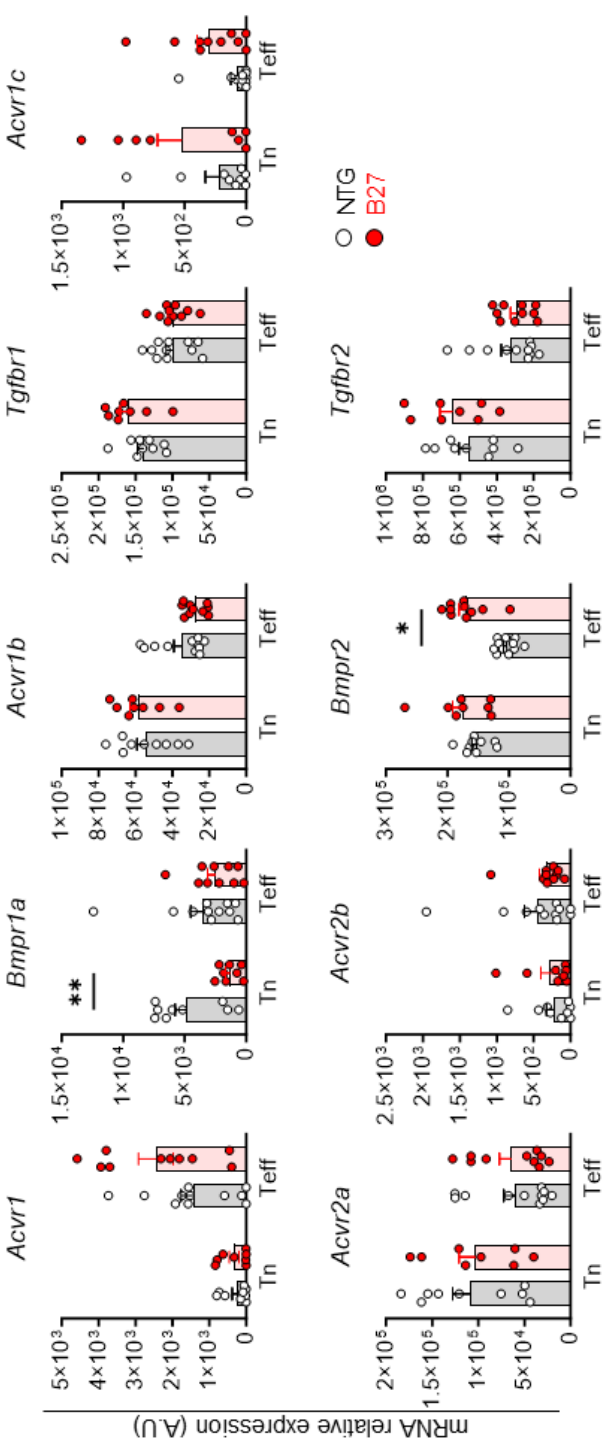

Lauraine et al., Figure 3

Figure 3

BMP/TGFb pathway receptors expression in Tn and Teff from B27 and NTG rats. The mRNA expression of TGFb and activin receptor genes was assessed by RT-qPCR in *ex-vivo* sorted Tn and Teff from NTG (grey bar – white dots) and B27 (red bar – red dots) adult rat mLNs. Scattered dot plot with bars represents the mean of mRNA relative expression in arbitrary units (A.U) out of 8 to 11 experiments. Differences between NTG and B27 expression levels for each receptor were tested by unpaired t-tests with Welch's correction (**: $p<0.01$). Error bars show SEM. On the first row *Acvr1*, *Bmpr1a, Acvr1b, Tgfbr1 and Acvr1c* genes coding for ALK2, ALK3, ALK4, ALK5 and ALK7 BMPR1s respectively. On the second row *Acvr2a, Acvr2b, Bmpr2 and Tgfbr2* represent type 2 BMP receptor genes.

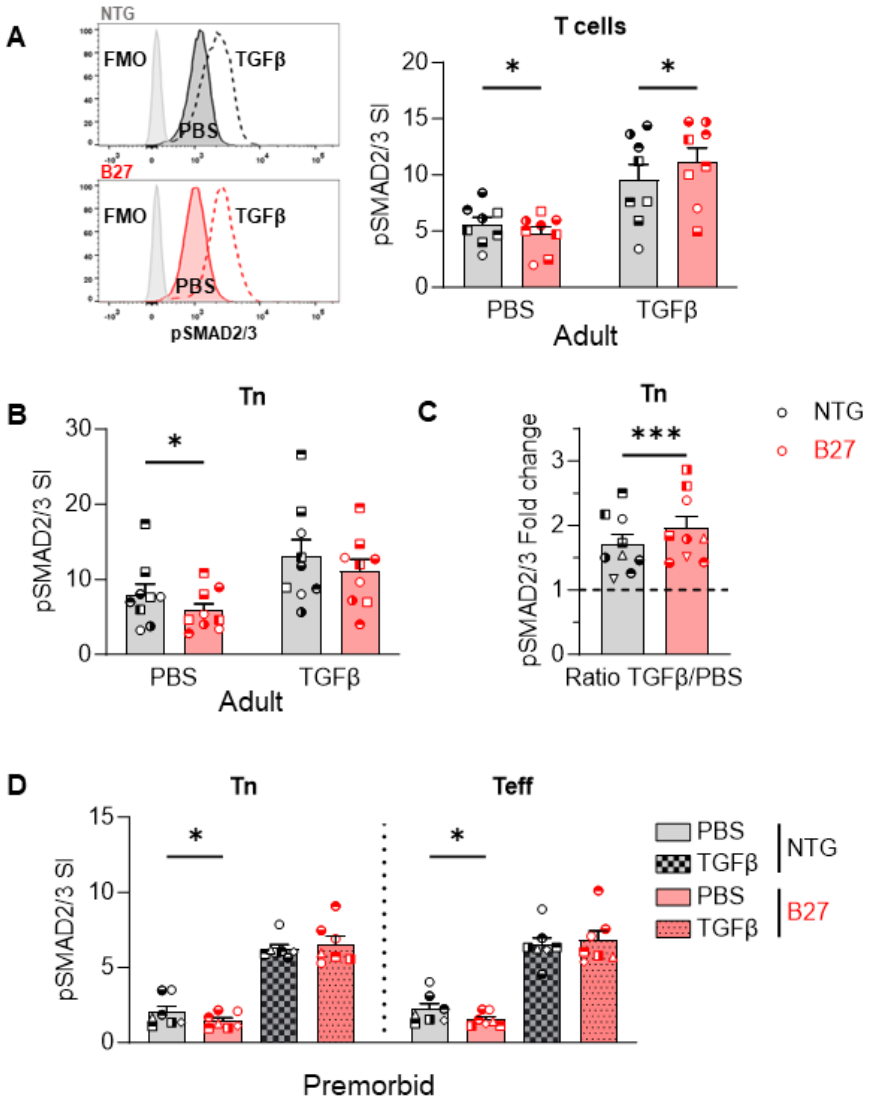

Lauraine et al., Figure 4

Figure 4

Basal pSMAD2/3 is reduced in B27 rat T cells but increases more after TGFβ1 stimuation. (A) Left: Representative histograms of pSMAD2/3 expression in mLN T cells from NTG and B27 rats after 1 hour exposure to medium alone (PBS) or TGFβ1 at 37°C. Right: Intracellular pSMAD2/3 was quantified in mLN T cells from B27 and NTG adult rats after exposure to TGFβ1 or medium alone. Scatter dot plots with bars representing the mean of the SI of 8 experiments. Similar symbols indicate paired conditions.

Vertical error bars show the SEM. Paired t-test *: p<0.05. (B,C) Intracellular pSMAD2/3 was quantified in Tn from B27 and NTG adult rats after exposure to medium (PBS) or TGFβ1 in 9 independent experiments. Similar symbols indicate paired conditions. (B) Bars height shows the SI mean values. Vertical error bars show the SEM. Paired t-test *: p<0.05. (C) Mean of pSMAD2/3-fold change after exposure to TGFβ expressed as the ratio of pSMAD2/3 SI after TGFβ1 stimulation over the SI without exposure from (B). Paired t-test ***: p<0.001, (D) Intracellular pSMAD2/3 was quantified after TGFβ1 stimulation or no stimulation by gating on Tn or Teff from premorbid NTG and B27 rats. Scatter dot plots with bar show the pSMAD2/3 SI. Similar symbols indicate paired conditions. Bars height show the SI mean values (n=7-9 independent experiments). Vertical error bars show the SEM. Paired t-test *: p<0.05.

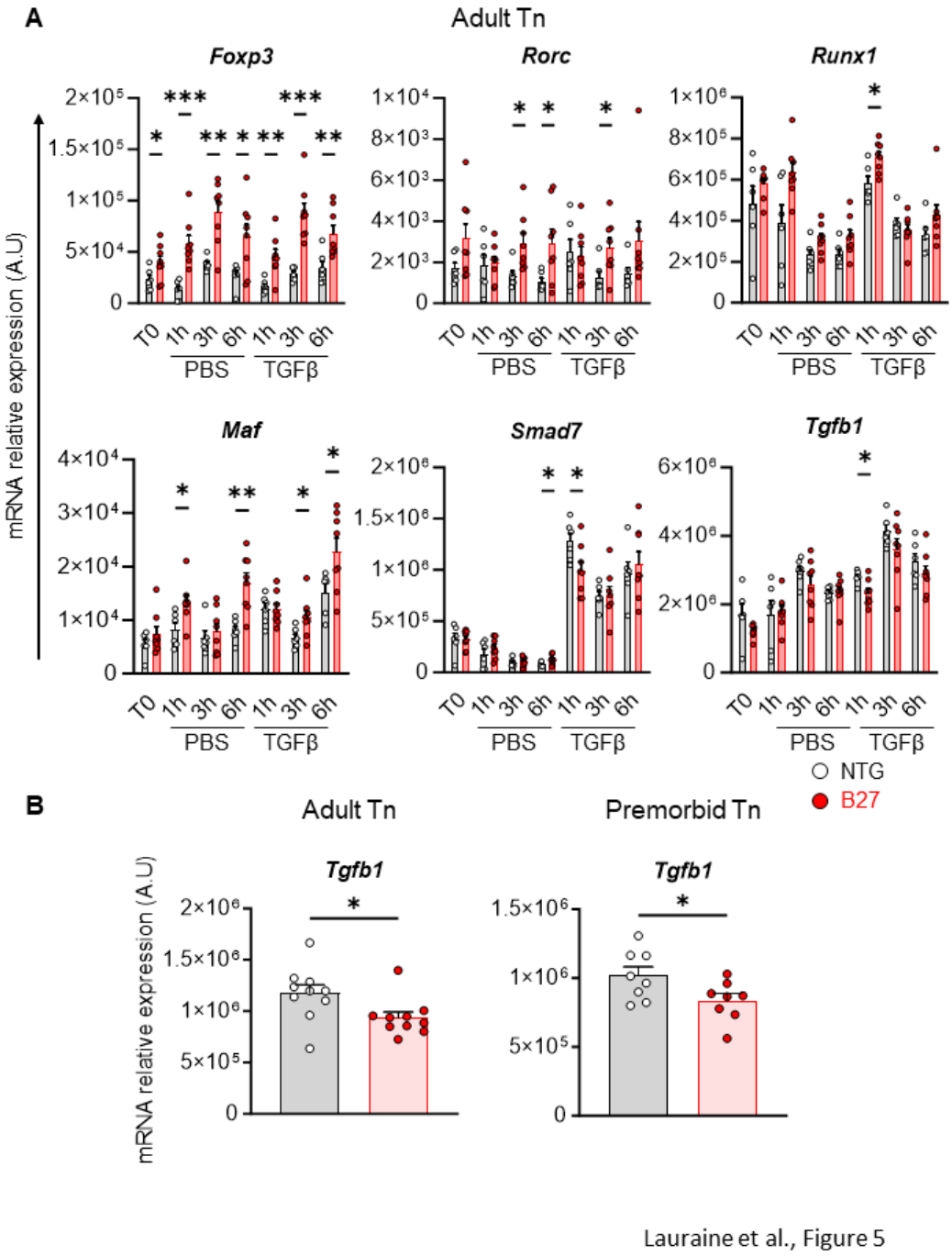

Lauraine et al., Figure 5

Figure 5

TGFβ target genes are differentially expressed between NTG and B27 rat Tn. (A) mRNA relative expression in mLN-sorted Tn from NTG (grey bar – white dots) or B27 (red bar – red dots) adult rats immediately after sorting (T0) or after 1h, 3h and 6h of incubation, without (PBS) or with TGFβ1, assessed by RT-qPCR. Scattered dot plots with bars show the mean of the mRNA relative expression out of 6 NTG and 8 B27 experiments. (B) *Tgfb1* mRNA relative expression in *ex-vivo*sorted Tn from NTG and

B27 adult (left panel) and premorbid (right panel) rats was assessed by RT-qPCR. Scattered dot plot with bars show the mean of mRNA relative expression out of 10 experiments for adult rats and 8 experiments for premorbid rats. In all graphics, differences between NTG and B27 expression level was tested by Welch's t-tests,*: $p<0.05$; **: $p<0.01$; ***: $p<0.001$.

Supplementary Files

This is a list of supplementary files associated with this preprint. Click to download.

- S1.png
- S2.png
- SupplementaryTables.docx